0° binary encounter electron production in 30-MeV O^{q+} + H_2, He, O_2, Ne, and Ar collisions

T. J. M. Zouros*
Physics Department, University of Crete and Institute of Electronic Structure & Laser, P.O. Box 2208, 710 03, Heraklion Crete, Greece

K. L. Wong,† S. Grabbe, H. I. Hidmi,‡ P. Richard, E. C. Montenegro,§ J. M. Sanders,‖ C. Liao,¶ S. Hagmann, and C. P. Bhalla
J. R. Macdonald Laboratory, Kansas State University, Manhattan, Kansas 66506
(Received 5 December 1994; revised manuscript received 6 November 1995)

Double-differential cross sections (DDCS's) for the production of binary encounter electrons (BEE's) were measured for collisions of 30-MeV O^{q+} projectiles with H_2, He, O_2, Ne, and Ar targets with $q=4-8$ and an electron ejection angle of $\theta=0°$ with respect to the beam direction. Particular interest focused on (a) the evaluation of the contributions of the different electron subshells of the multielectron targets, O_2, Ne, and Ar; (b) the study of the well-known enhancement of the BEE DDCS's with decreasing projectile charge-state q; here this dependence was tested for higher collision energies and new targets; (c) the study of the dependence of the BEE *peak energy* on the particular target and projectile charge state. Results were analyzed in terms of the impulse approximation, in which target electrons in the projectile frame undergo 180° elastic scattering in the field of the projectile ion. The electron scattering calculations were performed in a partial-wave treatment using the Hartree-Fock model. Good agreement with the data was found for the H_2 and He targets, while for the multielectron targets O_2, Ne, and Ar only electrons whose velocity was lower than the projectile velocity needed to be included for good agreement. All measured BEE DDCS's were found to increase with decreasing projectile charge state, in agreement with other recent BEE results. The BEE peak energies were found to be independent of the projectile charge state for all targets utilized.

PACS number(s): 34.70.+e, 34.50.Fa

I. INTRODUCTION

Binary encounter electrons (BEE's) [1–6] are target electrons ionized through direct, hard collisions with energetic projectiles, giving rise to a peak with a broad energy distribution. Since most of these electrons are produced at distances well within the K shell of the projectile ion, measurements of BEE double-differential cross sections (DDCS's) in both angle and energy can provide important information about dynamics of small impact parameter collisions and projectile screening [6–8]. A detailed understanding of BEE production is also useful in the study of K–Auger-electron spectra in heavy ion-atom collisions, since BEE production is often the dominant component of such spectra and can even interfere with coherent Auger electrons from other processes, such as resonant transfer excitation (RTEA) [9,10]. Furthermore, the BEE peak, because of its prominent appearance in all energetic heavy ion-atom electron spectra, can also be used for practical *in situ* absolute electron efficiency calibrations [11], thus providing a useful laboratory tool. Finally, one of the largest sources of damage in ion-dense-target collisions comes from BEE's. Thus consideration of the correct modeling of the projectile charge-state dependence of BEE production can be of direct importance to a variety of related fields ranging from heavy ion radiotherapy to the hardening of semiconductors produced in space against various types of radiation [12].

Studies in the 1970s utilizing *bare* projectiles showed that the BEE peak is well described by a variety of classical, semiclassical, and quantum formulations [4,13,14] of elastic scattering of target electrons off the bare projectile ion, establishing the well-known scaling of the BEE DDCS's, with the square of the projectile nuclear charge, Z_p^2. Similar studies of BEE production by *nonbare* projectiles showed the same framework could also be applied in this case, with the additional projectile electrons merely assumed to screen the Coulomb field of the projectile nuclear charge. The DDCS's then should scale with the effective (screened) projectile nuclear charge squared, $Z_p^{2\star}$ [6–8]. Measured BEE production data taken at 25° with respect to the beam direction in 30-MeV O^{q+} + O_2 collisions [5] were found to *decrease* with decreasing projectile charge state q, as expected from the static screening model [6,8].

Recent measurements, however, of BEE DDCS's at $\theta=0°$ from energetic collisions between nonbare projectiles and H_2 and He targets [15] have in fact shown the *opposite* projectile charge-state behavior to be true, i.e., the BEE DDCS's were found to *increase* with decreasing projectile charge state, contrary to all static screening expectations. This unexpected result generated a flurry of investigations

*Electronic address: tzouros@physics.uch.gr
†Present address: Lawrence Livemore National Laboratory, P.O. Box 808, Livermore, CA 94550.
‡Present address: Physics Department, Birzeit University, Birzeit–West Bank, Palestine.
§Permanent address: Dept. de Fisica, Pontificia Universidade Católica do Rio de Janeiro, Caixa Postal 38071, Rio de Janeiro 22453, Brazil.
‖Present address: Bldg. 5500 Ms-6377, Oak Ridge National Laboratory, P.O. Box 2008 Oak Ridge, TN 37831-6377.
¶Present address: Jet Propulsion Laboratory, MS 121-104, 4800 Oak Grove Drive, Pasadena, CA 91109-8099.

[10,16–27,12,28–56] leading to a new understanding of the BEE production mechanism. The experimental DDCS's for BEE production from fast collisions of ions with H_2 and He targets can be described within the impulse approximation (IA) as elastic scattering of quasifree electrons in the field of the projectile ion [16–18]. Electron exchange in the calculation of electron elastic differential cross sections is also found to be important [19,28,57,27], as was pointed out by Taulbjerg [19], and extensive theoretical results were presented in Ref. [27]. González *et al.* [32] and Hidmi *et al.* [40] experimentally investigated the effect of exchange for various collision systems and excellent agreement between theory and experiment was found only when exchange was included in the calculations.

The projectile charge-state dependence of the BEE DDCS's, following the results of Richard *et al.* [15], has been measured for a variety of collision systems using H_2 and He targets at both $\theta=0°$ [23–25,32,39,55] and $\theta\neq 0°$, [36,58,44,47] and calculated [20,21,12,29,27,22,28]. Both experiments and calculations confirm this general behavior. In fact, the projectile charge-state dependence is found to reverse itself around a critical laboratory observation angle θ_c (for O^{q+} projectiles $\theta_c=32°$), which is roughly independent of collision energy and projectile charge state [58,44,27]. For $\theta<\theta_c$ the DDCS's increase with decreasing projectile charge state, while for $\theta>\theta_c$ the DDCS decrease with decreasing projectile charge state.

Interest has also focused on the energy shift, $\Delta E\equiv 4t-E_{\rm peak}$, of the BEE distribution peak energy $E_{\rm peak}$ and its dependence on q. In a classical two-body collision between a *free* electron and a projectile ion, the BEE peak for an observation angle of 0° is independent of q appearing at an energy $4t$, where $t=\frac{1}{2}mV_p^2$ is the energy of an electron moving with the velocity of the projectile, V_p. For *bound* electrons, however, ΔE may depend sensitively on q and Z_t [11,26,59,34,41,43,60–62], reflecting two-center effects [63,64] arising from the simultaneous attraction of the ejected electrons from both the projectile and target. Thus measurements of ΔE for different targets and projectile charge states can test different models describing BEE production [26,59,35,34,41,48,43,49–51,65,60,62,61].

In this paper we investigate BEE production at $\theta=0°$ for 30-MeV O^{q+} projectiles with $q=4-8$, in collision with a variety of targets, including both the well-understood H_2 and He targets, as well as multielectron targets such as O_2, Ne, and Ar. Some results pertaining to the projectile charge-state dependence of the 30-MeV $O^{q+}+O_2$ BEE DDCS's have already been reported [45] and are not included.

Here, we also explore the role of the different target electron subshells contributing to BEE production, when using multielectron targets such as O_2, Ne, and Ar in addition to reporting results for BEE production with H_2 and He targets. The validity criterion for the IA requires that the velocity of the participating target electrons v must be much smaller than the projectile velocity V_p [11,66,45]. Clearly, there exist collision systems for which the inner shells will not always fulfill this criterion. For the present collision systems of 30-MeV $O^{q+}+O_2$, Ne, and Ar, the oxygen and neon K shells, as well as the argon K and L shells, do not fulfill the IA validity criterion. It is thus of interest to test the performance of the IA for BEE production with these heavy targets, particularly since for the much lighter H_2 and He targets the agreement between theory and experiment is exceedingly good, not only in the shape of the DDCS's, but also in their absolute magnitude. Furthermore, by extending the study of BEE production to heavier targets, we can also investigate the energy shift ΔE [26,59,41], as a function of q, so far studied only for H_2 and He targets.

Following a brief description of the experiment in Sec. II, the analysis of multielectron target BEE production within the IA is discussed in Sec. III. In Sec. IV the experimental results are compared to theory.

II. EXPERIMENT

The experiment was performed with highly charged ion beams obtained from the Kansas State University 7-MV Tandem Van de Graaff accelerator using the same 0° electron spectroscopy apparatus already described in detail in previous publications on BEE DDCS measurements [15,11,45].

Single-collision conditions for BEE production were carefully maintained. This required using the doubly differentially pumped 10-cm-long gas cell at pressures between 2 and 5 mTorr for the O_2 and Ne targets and between 1 and 2 mTorr for Ar. BEE measurements using H_2 and He targets could be performed at the higher target pressures of 20–40 mTorr [15,11].

The beam-induced background was reduced by carefully collimating the beam. Such a background, produced mainly by electrons scattered by the beam at the edges of the spectrometer slits and gas cell apertures, can be a large source of error at 0° observation [67]. This beam-induced electron background was directly determined by taking an electron spectrum without gas in the target cell. It was subsequently subtracted from the BEE spectrum with gas. The statistical error bars shown in the following figures arise mainly from this subtraction.

All BEE DDCS's were normalized to our measured 30-MeV $O^{8+}+H_2$ BEE DDCS at 0°. These latter DDCS's were, in turn, normalized to theoretical IA BEE DDCS's for this collision system as discussed in more detail in Sec. III B. All pressure readings were performed using the same MKS Baratron capacitance manometer to within an accuracy of 3%. The temperature variation of the gas cell utilized, as monitored in older tests using a thermocouple, were never larger than 5% and usually about 3%. Projectile charge normalization during measurement and from one measurement to the next was always accomplished assuming negligible charge exchange of the projectile beam during the collision. A shielded Faraday cup with electron suppression was used with a beam current integrator having an accuracy of 2–3 %. Thus the overall error from these sources of uncertainty is estimated to be less than 7%. Combining this uncertainty with the additional statistical error due to background subtraction, mentioned above, gave an overall absolute uncertainty of about 10–13 %.

III. ANALYSIS OF THE BINARY ENCOUNTER ELECTRON SPECTRA

The analysis of the BEE DDCS's entailed the correct absolute normalization of the experimental data and the deter-

TABLE I. The binding energies I and kinetic energies K of the targets utilized are listed below in eV. Results are taken from Ref. [76]. Binding energies are experimental data, while kinetic energies are calculated from nonrelativistic Hartree-Fock wave functions. Also listed is the IA validity parameter $\eta = V_p/v$, computed from $K = \frac{1}{2}mv^2$ and $V_p = 8.66$ a.u., the velocity of the projectile for 30-MeV collision energy.

Subshell	He			Ne			Ar		
	I	K	η	I	K	η	I	K	η
1s	24.59	39.51	5.06	866.9	1259.1	0.901	3203.0	4192.9	0.494
2s				48.47	141.88	2.68	320.0	683.1	1.22
2p				21.60	116.02	2.97	245.9	651.4	1.25
3s							29.24	103.5	3.14
3p							15.82	78.07	3.62

mination of the contributing target electron sub shells. Both procedures require the use of the IA and thus we discuss this first. The IA treatment of BEE production discussed here [11] is based on a model first applied to RTE [68]. Similar analyses have been used in the past to discuss the electron loss peak [69], BEE production from solids [70,71], and double-differential probabilities for electron emission as a function of impact parameter [72].

A. BEE production and the impulse approximation

The impulse approximation [68,70,11] approach, valid for $\eta \equiv V_p/v \gg 1$, v and V_p being the target electron and projectile velocities, respectively, gives the laboratory BEE DDCS's, $d^2\sigma/d\epsilon d\Omega$ for $\theta = 0°$ observation [11,73]:

$$\left(\frac{d^2\sigma}{d\epsilon d\Omega}\right)(\epsilon, \theta = 0°, q) = \frac{d\sigma}{d\Omega'}(\epsilon', \theta' = 180°, q) \times \sqrt{\frac{\epsilon}{\epsilon'}} \sum_i \frac{n_i J_i(p_{z_i})}{V_p + \frac{p_{z_i}}{m}}. \quad (1)$$

The single-differential cross section (SDCS) $d\sigma/d\Omega'(\epsilon', \theta', q)$ is that for a *free* electron with energy ϵ', elastically scattering off the projectile ion of charge q through an angle θ'. We note that $0°$ observation ($\theta = 0°$) corresponds to scattering through $\theta' = 180°$ in the projectile rest frame [11], for which the electron energies transform according to [11]:

$$\epsilon' = (\sqrt{\epsilon} - \sqrt{t})^2, \quad (2)$$

where ϵ' and ϵ are the electron energies in the projectile and laboratory rest frames, respectively, t is the cusp energy equal to $\frac{1}{2}mV_p^2$, and m is the mass of the electron.

The SDCS $d\sigma/d\Omega'(\epsilon', \theta', q)$ for a *bare* ion is just equal to the Rutherford SDCS, while for nonbare ions it must be calculated independently. A Hartree-Fock calculation of the nonbare ionic potential (including exchange) was performed and the elastic SDCS was then calculated in a partial-wave treatment. Details of such a calculation are given in Refs. [18,27]. Here these calculations were performed for various electron energies ϵ' and ionic potentials for all the O^{q+} ions utilized.

The z component of momentum, p_{z_i}, of an electron in the ith target subshell in the laboratory frame is given as a function of t, ϵ' and its binding energy I_i in the IA as [11,73]

$$p_{z_i} = \sqrt{2m}(\sqrt{\epsilon' + I_i} - \sqrt{t}). \quad (3)$$

The Compton profile $J_i(p_{z_i})$ represents the distribution in p_{z_i} of the n_i electrons in the ith target electron subshell. For H_2 and He, experimentally measured Compton profiles were used [74]. In the case of O_2, Ne, and Ar the tabulated values for the Compton profiles [75] were used in the calculation. The binding energies I_i are obtained from Ref. [76] and are listed in Tables I and II.

B. Absolute normalization of experimental BEE DDCS's

The absolute DDCS scale was determined by normalizing the experimental 30-MeV $O^{8+} + H_2$ BEE DDCS to the results of the IA calculation, thus calibrating the overall efficiency of electron detection in this electron-energy range as discussed in detail in Refs. [11,73]. Once the overall absolute electron detection efficiency has been determined it is assumed fixed for all subsequent measurements. This has proven to be an easy and accurate way of determining the *in situ* overall absolute electron detection efficiency of our apparatus [11].

The $O^{8+} + H_2$ normalization spectrum is shown in Fig. 1, where the experimental BEE DDCS is seen to fit the IA results extremely well. In Fig. 1 we also show the BEE DDCS for the case of bare projectiles in collision with all the other targets. As can be seen, the IA is also found to be in

TABLE II. Same as in Table I.

Subshell	H_2			O_2		
	I	K	η	I	K	η
$1\sigma_g$	15.43	31.96	5.65	543.5	794.84	1.13
$1\sigma_u$				543.5	795.06	1.13
$2\sigma_g$				40.3	78.19	3.62
$2\sigma_u$				25.69	90.40	3.36
$1\pi_u$				18.88	72.24	3.76
$3\sigma_g$				16.42	60.08	4.12
$1\pi_g$				12.07	82.14	3.53

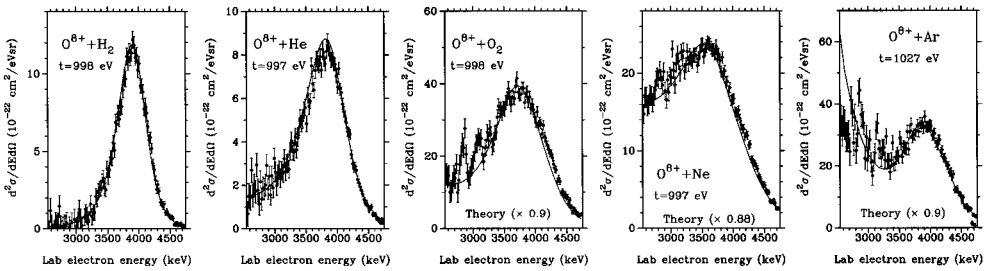

FIG. 1. 0° laboratory BEE DDCS's for *bare* 30-MeV O^{8+} collisions. The solid lines are the IA results. Experimental results have been normalized to the IA results of 30-MeV $O^{8+} + H_2$. The observed peaks to the left of the BEE peak is due to projectile KLL-Auger electrons. The cusp energy t, which was used to obtain the projectile velocity, is indicated in each spectrum (see text).

extremely good agreement with the He data in both shape and magnitude, while good agreement is observed in the case of the multielectron targets, when *only* target electrons from subshells with $\eta > 1$ are included in the calculation. A discussion of the contributions from the various subshells is given in the next section.

C. Determination of contributing target subshells

The number of target electrons per ith subshell, n_i, participating in the production of BEE's appearing in Eq. (1) needs to be determined. As mentioned earlier, the IA is applicable when $\eta_i \equiv V_p/v_i \gg 1$. The parameter η_i computed for the 30-MeV collision energy and the target electrons utilized are listed in Tables I and II. Both electrons of H_2 and He have η values larger than 5 (see Tables I and II), clearly satisfying the above IA applicability criterion. Thus, for these cases, $n=(2)$. However, the K-shell electrons of Ne and Ar are seen to have $\eta < 1$, while the K-shell electrons of O_2 and the L-shell electrons of Ar have $\eta > 1$ but just marginally so. Clearly, the IA criterion $\eta \gg 1$ is not met in these cases. In Fig. 2 we successively include the different subshells in the IA calculations and thereby obtain the configurations that give the best agreement with the data.

We have thus determined, using the values of η of Tables I and II and the bare ion results of Fig. 2, that the $2s^2 2p^4$ and $2s^2 2p^6$ configurations are the active target configurations for oxygen and neon, respectively, while for the argon target it is seen that the $2p^6 3s^2 3p^6$ configuration is in best agreement with the experimental results. Thus for the case of oxygen, $n=(0,2,4)$, for Ne, $n=(0,2,6)$, and for Ar, $n=(0,0,6,2,6)$, where the definition of the occupation vector is $n=(n_{1s}, n_{2s}, n_{2p}, n_{3s}, \ldots)$. In the case of O_2, the calculated atomic oxygen Compton profiles for the L-shell configurations were multiplied by 1.9 to reproduce earlier measured L-shell *molecular* oxygen Compton profiles [77,78]. We have chosen to present the IA results by scaling them to the high energy side of the measured BEE peaks. At these electron energies, possible contamination from the high energy tail of the cusp is minimized. The various scaling fac-

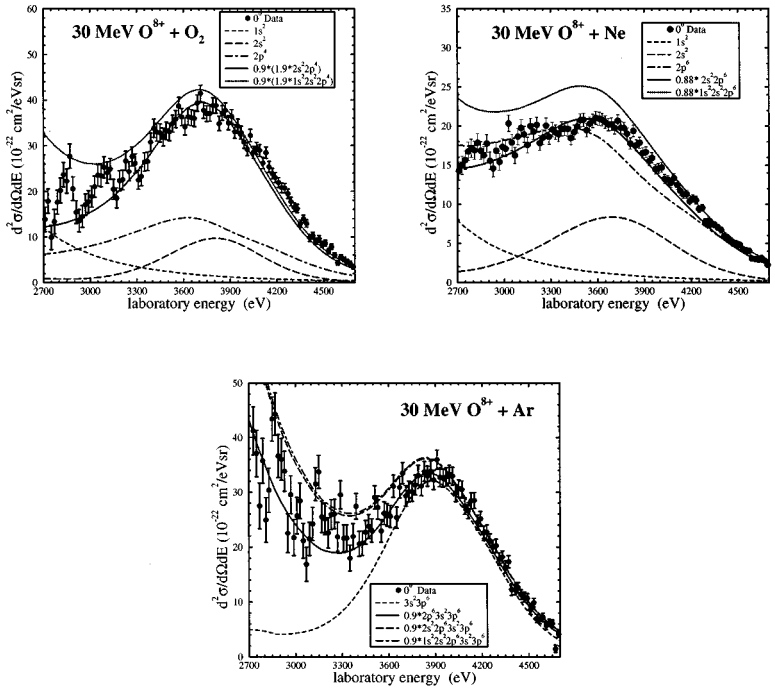

FIG. 2. 0° laboratory BEE DDCS's for *bare* 30-MeV O^{8+} collisions with O_2, Ne, and Ar targets. The various lines are the IA results for contributions from different target electron configurations. Experimental results have been normalized to the IA results of 30-MeV $O^{8+}H_2$. The observed peaks to the left of the BEE peak is due to projectile KLL-Auger electrons.

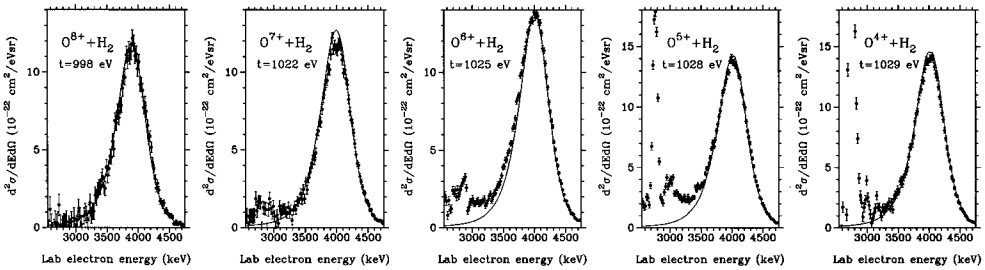

FIG. 3. 0° laboratory BEE DDCS's for 30-MeV $O^{q+} + H_2$ collisions. The solid lines are the IA results. Experimental results have been normalized to the IA results of 30-MeV $O^{8+} + H_2$. The observed peaks to the left of the BEE peak is due to projectile *KLL*-Auger electrons. The Cusp energy t, which was used to obtain the projectile velocity, is indicated in each spectrum (see text).

tors are mentioned explicitly in each figure. Finally, it was assumed that once the values of n_i are set using the bare projectile BEE DDCS, they remain the same for all other projectile charge states q. As already shown in Fig. 1, the IA calculations for O_2, Ne, and Ar used the above specifications of n.

D. Presentation of BEE DDCS's

We present our measured BEE laboratory DDCS's from the five different targets in Figs. 3–6. Also included in the figures are the IA results of Eq. (1) with n set as discussed above. Uncertainty in the precise experimental value of t (only roughly determined in these measurements) demanded that different values of t be used in the calculation of the BEE DDCS's for optimal results. Thus, in the IA calculation of the BEE DDCS's, t was chosen so that the computed BEE maximum was in good agreement with experiment. Small variations in t have negligible effect on the computed DDCS values.

IV. DISCUSSION

A. Comparison of BEE DDCS's with the IA

The BEE DDCS's for H_2 and He targets are shown in Figs. 3 and 4 to be in excellent overall agreement in both the shape and the height of the BEE peak for all projectile charge states. In the case of the multielectron targets shown in Figs. 5 and 6 agreement around the BEE peak, where the IA is valid, is also quite impressive. For the O_2 target (reported in Ref. [45]) the agreement is almost as good as for He. For the Ne target, however, the agreement in both the shape and the height of the BEE peak is poorer, especially in the case of projectile charge states $q=4$ and $q=5$, for reasons not understood. For the Ar target agreement is better than for Ne, with the exception of projectile charge state $q=5$ for which theory seems to be a bit larger and slightly broader than the measured BEE peak.

For *bare* projectiles, as seen in Fig. 1, the IA gives very good agreement with experiment for the H_2 and He targets, but needs to be scaled by 0.88 for Ne and by 0.9 for O_2 and Ar. For *nonbare* projectiles, similar scaling factors are also required, as seen from the comparison of the IA to the experimental data shown in Figs. 4–6. We note that multiple target ionization is well known to occur at these collision energies [79,80]. The ratio R_{21} of total double-to-single ionization is known to increase with increasing projectile charge state and decreasing collision energy. For example, for 1.84-MeV/u O^{8+} on He, $R_{21}=0.125$ [80]. This ratio could become even larger in the case of multielectron targets, as shown in the work of Haugen *et al.* [79]. To date, the effect of multiple ionization on electron DDCS's has not been studied, all existing data being based on *total* cross section measurements. Multiple target ionization will clearly reduce the BEE peak and might also affect its shape. More work in this direction is clearly desirable.

As shown by the visible K-Auger lines in the case of multielectron targets (see Fig. 1), electron capture is clearly not negligible and could thus be responsible for the reduction of the BEE peak. Projectile electron loss could also have some bearing. However, a quick estimate shows these effects to be small; electron capture and electron loss can take place in the beam line prior to the target or in the target itself. The beam line pressure was always less than 5×10^{-7} Torr, thus offering an effective areal density of $\sim2\times10^{13}$ molecules/cm^2 for a beam line length of 1050 cm. Target pressures in the case of Ar were about 2 mTorr, thus giving an effective areal density of $\sim7.8\times10^{14}$ molecules/cm^2 for a target cell length of 10 cm. Electron loss cross sections for 30-MeV O^{q+} collisions in N_2 and Ar are smaller than 5×10^{-17} cm^2, while electron capture cross sections are

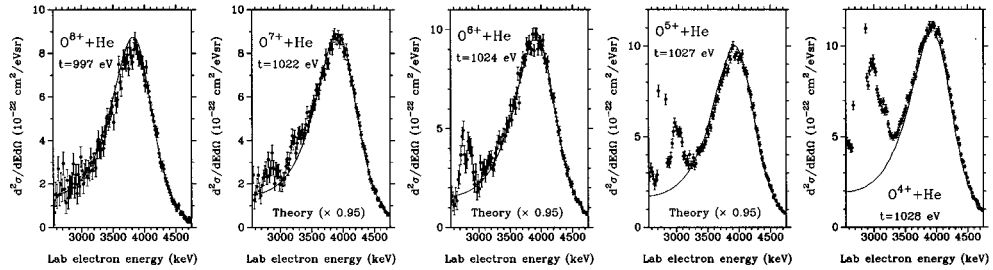

FIG. 4. Same as in Fig. 3 but for O^{q+} + He.

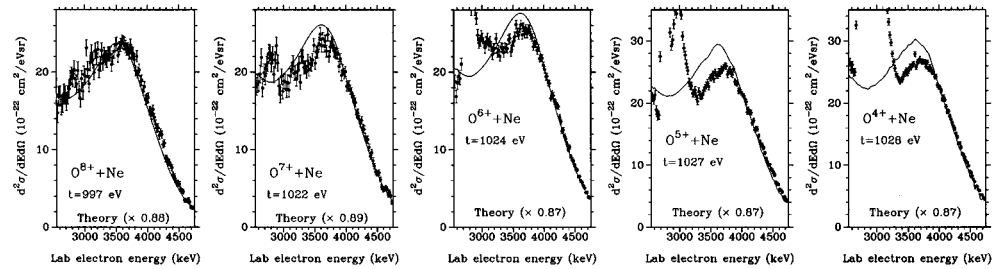

FIG. 5. Same as in Fig. 3 but for O^{q+} + Ne. The solid lines are the IA results from contributions of $2s$ and $2p$ target electrons only.

roughly one magnitude smaller [81]. Thus estimates show that in the worst case senario of electron loss for O^{4+} projectiles, less than 0.06% of the beam changes to O^{5+} in the beam line prior to the target, while less than 4% of the beam changes to O^{5+} in collisions with the Ar target, leading to errors of less than 1% in the determination of the DDCS's.

We note that the Ne Compton profile is the broadest of all the targets used and thus the experimental Ne BEE DDCS's were the least prominent and the most difficult to separate from the beam-induced background due to slit scattering, mentioned in the experimental section. The Ne data measurements were repeated at different beam times, but the BEE DDCS's were never found to vary by more than 10%.

In Fig. 7 we plot the ratio R of the BEE DDCS's for $q=4-8$ to that of $q=8$ at the maximum of the BEE peaks [15]. Errors in the determination of R arising from small shifts in the energy of the BEE peak maxima were negligible in the case of O_2 and Ne targets since these have much broader energy distributions than those for the H_2 and He targets. Clearly R is seen to increase as a function of decreasing q for all targets. This is also found to be the case for the calculation. All theoretical results are seen to be in good agreement with the experimental value of R, except in the case of Ne, which, as noted above, was also not in very good agreement as far as the shape of the DDCS's was concerned and thus disagreement between theory and experiment in the determination of R could even be fortuitous.

B. BEE peak energy

We plot the energy shift $\Delta E=4t-E_{\mathrm{peak}}$ for the five different targets utilized as a function of the projectile charge state in Fig. 8. E_{peak} is the *measured* energy at the peak of the BEE distribution [11,41]. As can be seen from the figure, *no* dependence of ΔE on the projectile charge state q is observed. However, a strong dependence on the target species is clearly observed.

The IA calculations presented using the Hartree-Fock model for the electron-ion scattering predict ΔE to be *independent* of the projectile charge state q, in good agreement with the above observations [41]. Other calculations, however, do show a dependence of ΔE on the projectile charge state q.

Estimates of the energy shift for *bare* projectiles ($q=Z_p$) are given in closed form by two simple models. The Bohr-Linhard model, in which the target electron has a release radius determined by its position at which the electrostatic attractions of both projectile and target cancel each other out, indicates a strong $q^{1/2}$ dependence of ΔE [59]:

$$\Delta E_{\mathrm{BL}}=2\sqrt{q}(2I)^{\frac{3}{4}}/Z_t^{\frac{1}{6}}\ \text{(a.u.)}, \tag{4}$$

where I is the ionization potential of the target listed in Table III.

The tunneling model (TM), in which the electron resonantly tunnels from the initial target bound state to a final projectile continuum state, as used by Fainstein *et al.* [34], also gives a similar $q^{1/2}$ dependence, but with a quite different dependence on I and Z_t:

$$\Delta E_{\mathrm{TM}}=2I+\sqrt{4qZ_t^3/3}\ \text{(a.u.)}. \tag{5}$$

We note that Eq. (5) has been derived for hydrogenic targets and is therefore not applicable in this form to multielectron targets.

We compare the measured shifts ΔE with those of the two models, ΔE_{BL} and ΔE_{TM}, for bare O^{8+} in collision with the various targets, in Table III. In these calculations, the ionization potential I of the outermost target electrons was used and no effort was made to account for the increased screening of the nuclear charge of the target Z_t for the multielectron targets, the energy shifts in Eqs. (4) and (5) being rather insensitive to the value of Z_t. As can be seen from Table III, agreement between theory and experiment is not good. The strong dependence of these models on $\sqrt{q}$ is

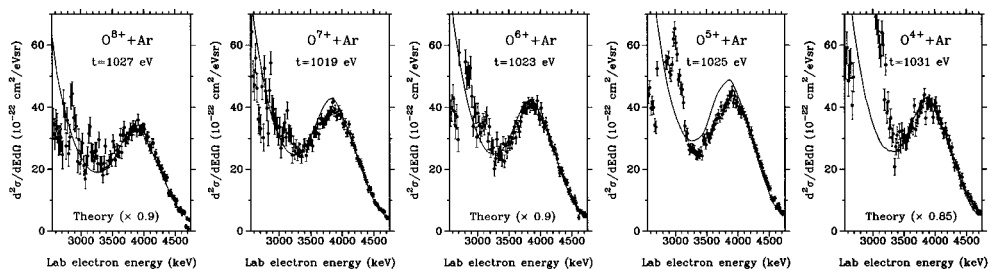

FIG. 6. Same as in Fig. 5 but for O^{q+} + Ar. The solid lines are the IA results from contributions of $2p$, $3s$, and $3p$ target electrons only.

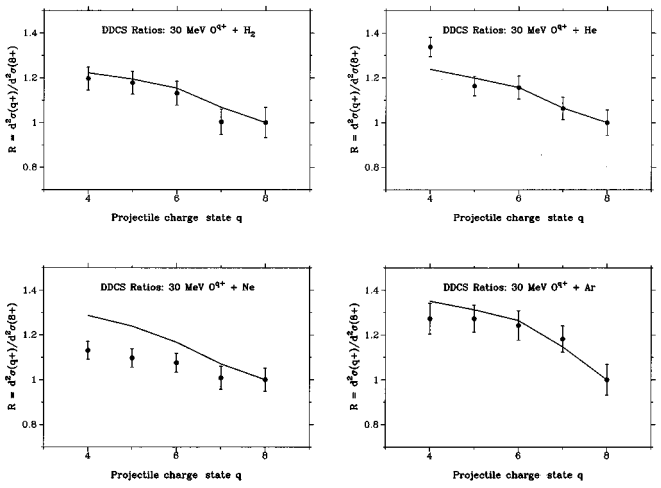

FIG. 7. Closed circles: Projectile charge-state dependence of BEE DDCS's relative to bare ion BEE DDCS's for 30-MeV O^{q+} + H_2, He, Ne, and Ar targets for 0°. Solid lines: IA results for $\theta=0°$ observation.

clearly not observed in our data. More sophisticated quantum and semiclassical calculations [26,34,43,65] have shown a milder dependence of ΔE on q and would probably give improved results.

Other recent experimental results [11] found ΔE to be 94 eV for collisions of *bare* F, O, N, and C ions at several projectile ion energies, and 37 eV for 1.5-MeV protons, all on H_2 targets. For bare F and protons at collision energies of 1.5 Mev/u with He targets, energy shifts of 174 eV and 82 eV were measured, respectively [11]. These results also support the IA results showing no dependence of ΔE on q. Our measured energy shifts for H_2 and He targets are seen to be in good agreement with those measured in Ref. [11]. Further investigations utilizing *nonbare* projectiles of various charge states in collisions with H_2 and He targets also found no q dependence of ΔE, for the case where $Z_p \leqslant 9$, in agreement with our own results for H_2 and He [40]. However, when heavier projectiles such as Si^{4-13+}, Cl^{5-13+}, and Cu^{4-15+} were used, a clear q dependence was observed [40]. Continuum-distorted-wave-eikonal-initial-state (CDW-EIS) calculations [34], explicitly including the influence of the projectile, are only in moderate agreement with these experimental results, mostly underestimating the energy shifts. Clearly, no existing model can accurately predict ΔE and its dependence on q.

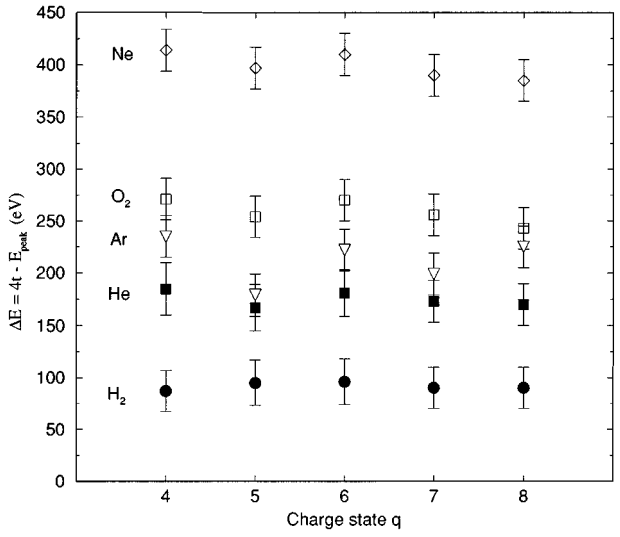

FIG. 8. Energy shifts $\Delta E=4t-E_{\text{peak}}$ (see text) as a function of projectile charge state q for 30-MeV collision of O^{q+} with H_2 (dark circles), He (dark squares), O_2 (open squares), Ne (open diamonds), and Ar (open triangles) targets. The measured energy shifts ΔE are listed in Table III for the case of *bare* ($q=8$) projectiles where they are compared to the theoretical shifts ΔE_{BL} and ΔE_{TM} computed from Eqs. (4) and (5).

TABLE III. Measured energy shifts $\Delta E=4t-E_{\text{peak}}$ (see text) for 30-MeV O^{8+} collisions with H_2, He, O_2, Ne, and Ar targets. Also given for comparison are the results for the energy shifts calculated by the Bohr-Linhard (BL) model [refer to Eq. (4)] and the tunneling model (TM) [refer to Eq. (5)]. All energies are in eV.

Target	I	ΔE	ΔE_{BL}	ΔE_{TM}
H_2	15.43	90 ± 20	169	120
He	24.59	170 ± 20	214	301
O_2	12.07	243 ± 20	99	
Ne	21.60	385 ± 20	148	
Ar	15.82	225 ± 20	106	

V. SUMMARY AND CONCLUSION

We have measured binary encounter electron production in 30-MeV O^{q+} projectiles in collision with H_2, He, O_2, Ne, and Ar targets, as a function of projectile charge state $q=4-8$, at 0° with respect to the beam direction. Calculated BEE DDCS's based on the impulse approximation and independently computed elastic electron scattering cross sections were found to be in excellent agreement with the data for H_2 and He targets, and in good agreement for the other multielectron targets, but only when subshells with $\eta>1$ were included.

All measured BEE DDCS were found to increase with decreasing projectile charge state q in agreement with all recent results in the literature. Theoretical calculations of the q dependence of the DDCS were also in excellent agreement for all targets investigated, except Ne. For the Ne target, less than satisfactory agreement was found for reasons not well understood. Furthermore, it was demonstrated that in the case of the multielectron targets O_2, Ne, and Ar, only the outer subshells should be included in the impulse approximation calculation, for best agreement with experiment.

Energy shifts ΔE of the BEE peak as a function of projectile charge state q and target species were also determined and found to be in excellent agreement with the IA results in the case of H_2 and He targets, and in fair agreement for the other multielectron targets utilized. No q dependence of ΔE was observed.

ACKNOWLEDGMENTS

We acknowledge stimulating discussions with Bob Dubois and N. Stolterfoht. We are grateful to Tricia M. Reeves for carefully reading the manuscript. This work was supported by the Division of Chemical Sciences, Office of Basic Energy Sciences, Office of Energy Research, U.S. Department of Energy. T.J.M.Z. and P.R. would also like to acknowledge the support of NATO Collaborative Research Grant No. CRG-910567.

[1] M. E. Rudd and T. Jorgensen, Phys. Rev. **131**, 666 (1963).
[2] M. E. Rudd, C. A. Sauter, and C. L. Bailey, Phys. Rev. **151**, 20 (1966).
[3] T. F. M. Bonsen and L. Vriens, Physica **47**, 307 (1970).
[4] M. E. Rudd and J. H. Macek, in *Case Studies in Atomic Physics*, edited by E. W. McDaniels and M. C. McDowell (North-Holland, Amsterdam, 1972), Vol. 3, pp. 47–136.
[5] N. Stolterfoht *et al.*, Phys. Rev. Lett. **33**, 59 (1974).
[6] N. Stolterfoht, in *Topics in Current Physics, Vol. 5: Structure and Collisions of Ions and Atoms*, edited by I. A. Sellin (Springer-Verlag, Berlin, 1978), p. 155.
[7] J. H. McGuire, N. Stolterfoht, and P. R. Simony, Phys. Rev. A **24**, 97 (1981).
[8] L. H. Toburen, N. Stolterfoht, P. Ziem, and D. Schneider, Phys. Rev. A **24**, 1741 (1981).
[9] C. P. Bhalla, Phys. Rev. Lett. **64**, 1103 (1990).
[10] T. J. M. Zouros, P. Richard, and D. H. Lee, in *Proceedings of the 4th Workshop on High-Energy Ion-Atom Collision Processes, Debrecen, Hungary*, edited by D. Berényi and G. Hock (Springer-Verlag, Berlin, 1991).
[11] D. H. Lee *et al.*, Phys. Rev. A **41**, 4816 (1990).
[12] D. R. Schultz and R. E. Olson, J. Phys. B **24**, 3409 (1991).
[13] D. H. Madison, Phys. Rev. A **8**, 2449 (1973).
[14] S. T. Manson, L. H. Toburen, D. H. Madison, and N. Stolterfoht, Phys. Rev. A **12**, 60 (1975).
[15] P. Richard *et al.*, J. Phys. B **23**, L213 (1990).
[16] R. E. Olson, C. O. Reinhold, and D. R. Schultz, J. Phys. B **23**, L455 (1990).
[17] C. O. Reinhold, D. R. Schultz, and R. E. Olson, J. Phys. B **23**, L591 (1990).
[18] R. Shingal *et al.*, J. Phys. B **23**, L637 (1990).
[19] K. Taulbjerg, J. Phys. B **23**, L761 (1990).
[20] C. O. Reinhold *et al.*, Phys. Rev. Lett. **66**, 1842 (1991).
[21] C. O. Reinhold, D. R. Schultz, and R. E. Olson, Nucl. Instrum. Methods Phys. Res. Sect. B **56/57**, 271 (1991).
[22] Z. Chen, D. Madison, and C. D. Lin, J. Phys. B **24**, 3203 (1991).
[23] P. Hvelplund *et al.*, J. Phys. Soc. Jpn. **60**, 3675 (1991).
[24] T. B. Quinteros *et al.*, J. Phys. B **24**, 1377 (1991).
[25] O. Jagutzki *et al.*, J. Phys. B **24**, 2579 (1991).
[26] J. Miraglia and J. Macek, Phys. Rev. A **43**, 5919 (1991).
[27] C. P. Bhalla and R. Shingal, J. Phys. B **24**, 3187 (1991).
[28] A. Salin, J. Phys. B **24**, L611 (1991).
[29] T. Quinteros and J. F. Reading, Nucl. Instrum. Methods Phys. Res. Sect. B **53**, 363 (1991).
[30] K. Taulbjerg, J. Phys. B **24**, 1125 (1991).
[31] S. Hagmann *et al.*, J. Phys. B **25**, L287 (1992).
[32] A. D. González, P. Hvelplund, A. G. Petersen, and K. Taulbjerg, J. Phys. B **25**, L57 (1992).
[33] W. Wolff *et al.*, J. Phys. B **25**, 3683 (1992).
[34] P. D. Fainstein, V. H. Ponce, and R. D. Rivarola, Phys. Rev. A **45**, 6417 (1992).
[35] B. H. Bransden and M. R. C. McDowell, *Charge Exchange and the Theory of Ion-atom Collisions* (Clarendon Press, Oxford, 1992).
[36] D. H. Schneider *et al.*, Phys. Rev. A **46**, 1296 (1992).
[37] W. Wolff *et al.*, J. Phys. B **26**, L65 (1993).
[38] A. D. González, P. Dahl, P. Hvelplund, and P. D. Fainstein, J. Phys. B **26**, L135 (1993).
[39] Y. Kanai *et al.*, in *Proceedings of the VIth International Conference on the Physics of Highly-Charged Ions*, edited by M. Stockli, P. Richard, C. L. Cocke, and C. D. Lin (AIP, New York, 1993), p. 315.
[40] H. I. Hidmi *et al.*, Phys. Rev. A **47**, 2398 (1993).
[41] H. I. Hidmi *et al.*, Phys. Rev. A **48**, 4421 (1993).
[42] S. Hagmann *et al.*, Radiat. Eff. Defects Solids **126**, 35 (1993).
[43] P. D. Fainstein, L. Gulyás, and A. Salin, J. Phys. B **27**, L259 (1994).
[44] R. D. Dubois, L. H. Toburen, M. E. Middendorf, and O. Jagutzki, Phys. Rev. A **49**, 350 (1994).
[45] T. J. M. Zouros *et al.*, Phys. Rev. A **49**, 3155 (1994).
[46] N. Stolterfoht *et al.*, Phys. Rev. A **49**, 5112 (1994).
[47] C. Liao *et al.*, Phys. Rev. A **50**, 1328 (1994).
[48] J. N. Madsen and K. Taulbjerg, J. Phys. B **27**, 2239 (1994).
[49] D. H. Jakubaßa-Amundsen, Phys. Rev. A **49**, 2634 (1994).
[50] D. H. Jakubaßa-Amundsen, Nucl. Instrum. Methods Phys. Res. Sect. B **86**, 82 (1994).
[51] D. H. Jakubaßa-Amundsen, Z. Phys. D **34**, 9 (1995).
[52] J. H. Posthumus *et al.*, J. Phys. B **27**, L97 (1994).
[53] J. H. Posthumus *et al.*, J. Phys. B **27**, 2521 (1994).
[54] W. Wolff *et al.*, J. Phys. B **28**, 1265 (1995).
[55] J. M. Sanders *et al.* (unpublished)
[56] B. D. DePaola *et al.* (unpublished).
[57] V. H. Ponce, P. D. Fainstein, and R. D. Rivarola, J. Phys. B **26**, 1343 (1993).
[58] A. D. González, P. Dahl, P. Hvelplund, and K. Taulbjerg, J. Phys. B **25**, L573 (1992).
[59] J. O. P. Pedersen, P. Hvelplund, A. G. Petersen, and P. D. Fainstein, J. Phys. B **24**, 4001 (1991).
[60] N. Stolterfoht *et al.*, Phys. Rev. A **52**, 3796 (1995).
[61] N. Stolterfoht, in *Two-Center Effects in Ion-Atom Collisions*, edited by T. J. Gay and A. F. Starace, AIP Conf. Proc. No. 362 (AIP, New York, 1996), p. 69.
[62] P. Richard, in *Two-Center Effects in Ion-Atom Collisions* (Ref. [61]), p. 163.
[63] N. Stolterfoht, Phys. Rep. **146**, 315 (1987).
[64] P. D. Fainstein, V. H. Ponce, and R. D. Rivarola, J. Phys. B **24**, 3091 (1991).
[65] L. Gulyás, P. D. Fainstein, and A. Salin, J. Phys. B **28**, 245 (1995).
[66] E. C. Montenegro, W. E. Meyerhof, and J. H. McGuire, Adv.

At. Mol. Opt. Phys. **34**, 249 (1994).
[67] A. Itoh *et al.*, J. Phys. B **16**, 3965 (1983).
[68] D. Brandt, Phys. Rev. A **27**, 1314 (1983).
[69] D. Burch, W. Wieman, and W. B. Ingalls, Phys. Rev. Lett. **30**, 823 (1973).
[70] F. Bell, H. Böckl, M. Z. Wu, and H.-D. Betz, J. Phys. B **16**, 187 (1983).
[71] H. Böckl and F. Bell, Phys. Rev. A **28**, 3207 (1983).
[72] J. P. Hansen and L. Kocbach, J. Phys. B **22**, L71 (1989).
[73] T. J. M. Zouros, in *Recombination of Atomic Ions*, Vol. 296 of *NATO Advanced Study Institute Series B: Physics*, edited by W. G. Graham, W. Fritsch, Y. Hahn, and J. Tanis (Plenum, New York, 1992), pp. 271–300.
[74] J. S. Lee, J. Chem. Phys. **66**, 4906 (1977).
[75] F. Biggs, L. B. Mendelsohn, and J. B. Mann, At. Data Nucl. Data Tables **16**, 201 (1975).
[76] Y.-K. Kim, in *Physics of Ion-Ion and Electron-Ion Collisions*, Vol. 83 of *NATO Advanced Study Institute Series B: Physics*, edited by F. Brouillard and J. W. McGowan (Plenum, New York, 1983), pp. 101–166.
[77] P. Eisenberger, Phys. Rev. A **5**, 628 (1971).
[78] P. Eisenberger, W. H. Henneker, and P. E. Cade, J. Chem. Phys. **56**, 1207 (1972).
[79] H. Haugen, L. H. Andersen, P. Hvelplund, and H. Knudsen, Phys. Rev. A **26**, 1962 (1982).
[80] H. Knudsen *et al.*, J. Phys. B **17**, 3545 (1984).
[81] J. R. Macdonald and F. W. Martin, Phys. Rev. A **4**, 1965 (1971).